Reversed flow of Atlantic deep water during the Last Glacial Maximum

Reversed flow of Atlantic deep water during the Last Glacial Maximum

César Negre*, Rainer Zahn, Alexander L. Thomas, Pere Masqué, Gideon M. Henderson, Gema Martínez-Méndez, Ian R. Hall and José L. Mas

*Corresponding Author.

Supplementary Information

S1: Introduction to $^{231}Pa/^{230}Th$ as a water flow-rate proxy

Both ^{231}Pa and ^{230}Th are produced continually in the ocean water column from the decay of dissolved uranium at a fixed $^{231}Pa/^{230}Th$ activity ratio of 0.093. Differential solubility of the two isotopes in the ocean makes the sedimentary $^{231}Pa_{xs,0}/^{230}Th_{xs,0}$ ratio (*i.e.*, excess ^{231}Pa and ^{230}Th activity ratio decay corrected to the time of deposition, referred in the manuscript as $^{231}Pa/^{230}Th$) a powerful tool to study deep-water circulation and flow rates and, by extension, the MOC vigour (Marchal *et al.*, 2000). ^{230}Th is highly particle reactive and is scavenged from the water column by the particle flux more rapidly than ^{231}Pa, which resides in the water column long enough to be laterally transported by ocean currents. This is today illustrated by the southward flow of North Atlantic Deep Water, which exports about 50% of the ^{231}Pa produced in the Atlantic basin compared to only ~10% of the ^{230}Th (Yu *et al.*, 1996); the water column in this case becomes depleted in dissolved ^{231}Pa resulting in low $^{231}Pa/^{230}Th$ ratios in the underlying sediments. The faster the movement of the water mass, the lower will be the $^{231}Pa/^{230}Th$ ratios recorded on the bottom-floor. This water movement will be also recorded in sediments as a gradual increase of $^{231}Pa/^{230}Th$ ratios as we move downstream along the water mass pathway, until reaching equilibrium close to the production ratio value of 0.093 (Thomas et al., 2007).

S2: Estimation of $^{231}Pa/^{230}Th$ ratios in core MD02-2594.

Table S2-1. Raw ^{231}Pa, ^{230}Th, ^{232}Th, ^{238}U data (±1σ) of core MD02-2594, and resulting $^{231}Pa/^{230}Th$ ratios (details on the calculation procedure below in this section).

Core Depth (cm.)	Age (ka BP)*	^{231}Pa ($Bqkg^{-1}$)	^{230}Th ($Bqkg^{-1}$)	^{232}Th ($Bqkg^{-1}$)	^{238}U ($Bqkg^{-1}$)	$^{231}Pa_{xs,0}/^{230}Th_{xs,0}$
5-6	0.26	6.59 ± 0.16	110.0 ± 1.3	20.5 ± 0.3	34.67 ± 0.08	0.062 ± 0.002
15-16	0.83	6.4 ± 0.4	104 ± 8	19.2 ± 1.4	57.3 ± 0.8	0.064 ± 0.007
25-26	1.39	6.4 ± 0.2	103.2 ± 1.7	19.3 ± 0.3	49.95 ± 0.17	0.065 ± 0.003
35-36	1.96	6.9 ± 0.3	103 ± 7	18.7 ± 1.3	29.5 ± 1.5	0.071 ± 0.006
50-51	2.82	7.07 ± 0.15	99 ± 6	18.4 ± 1.1	41 ± 2	0.077 ± 0.005
65-66	3.86	6.22 ± 0.16	99 ± 5	18.7 ± 1.1	37 ± 2	0.068 ± 0.005
75-76	4.56	6.48 ± 0.12	96 ± 4	17.7 ± 0.7	53.5 ± 1.9	0.073 ± 0.004
85-86	5.26	6.1 ± 0.3	97 ± 6	18.1 ± 1.2	65 ± 4	0.068 ± 0.007
88-89	5.47		94 ± 4	17.5 ± 0.7	68 ± 2	
100-101	6.31	5.43 ± 0.10	93 ± 4	17.1 ± 0.7	46.6 ± 1.6	0.064 ± 0.003
115-116	7.29	5.28 ± 0.13	89 ± 4	17.0 ± 0.7	48 ± 2	0.066 ± 0.004
125-126	7.83	5.3 ± 0.2	89 ± 6	16.8 ± 1.2	44 ± 3	0.066 ± 0.007
135-136	8.37	4.66 ± 0.12	85 ± 3	16.3 ± 0.7	52 ± 3	0.060 ± 0.003
145-146	8.92	4.4 ± 0.4	85 ± 4	16.4 ± 1.2	41 ± 3	0.057 ± 0.007
155-156	9.46	4.26 ± 0.10	82 ± 6	15.2 ± 1.0	30 ± 2	0.058 ± 0.005
160-161	9.71		82 ± 3	13.9 ± 0.5	39.1 ± 1.4	
165-166	9.97	3.77 ± 0.09	81 ± 4	13.5 ± 1.0	51 ± 3	0.050 ± 0.003
175-176	10.56	3.66 ± 0.09	77 ± 2	12.8 ± 0.4	43.1 ± 1.5	0.051 ± 0.002
185-186	11.15	3.66 ± 0.10	79 ± 3	12.5 ± 0.6	40 ± 2	0.050 ± 0.003
195-196	11.74	3.9 ± 0.2	81 ± 5	12.2 ± 0.8	39 ± 2	0.054 ± 0.006
205-206	12.33	3.59 ± 0.08	82 ± 2	10.8 ± 0.3	66 ± 2	0.045 ± 0.002
215-216	13.08	3.47 ± 0.09	79 ± 2	10.5 ± 0.3	52.2 ± 1.8	0.047 ± 0.002
225-226	13.99	3.7 ± 0.3	81 ± 5	11.9 ± 0.9	48 ± 3	0.050 ± 0.006
235-236	14.90	3.51 ± 0.09	78 ± 2	11.1 ± 0.3	52.0 ± 1.8	0.049 ± 0.002
245-246	15.81	3.45 ± 0.09	80 ± 4	12.6 ± 0.9	55 ± 4	0.046 ± 0.004
255-256	16.94	3.0 ± 0.3	65 ± 3	11.4 ± 0.6	46 ± 2	0.050 ± 0.007
265-266	17.41	3.35 ± 0.14	68 ± 3	11.6 ± 0.7	48 ± 2	0.056 ± 0.005
270-271	17.65	2.71 ± 0.09	66 ± 3	11.1 ± 0.5	41.8 ± 1.5	0.044 ± 0.003
275-276	17.89	2.6 ± 0.2	66 ± 4	11.5 ± 0.8	56 ± 2	0.038 ± 0.006
285-286	18.36	2.45 ± 0.16	63 ± 3	12.0 ± 0.9	37.1 ± 1.4	0.042 ± 0.005
295-296	18.83	2.8 ± 0.2	65 ± 4	11.4 ± 0.7	44 ± 3	0.046 ± 0.007
305-306	20.75	2.74 ± 0.08	64 ± 3	12.0 ± 0.5	50.9 ± 1.8	0.045 ± 0.003
315-316	22.68	2.72 ± 0.08	67 ± 3	11.8 ± 0.7	49 ± 3	0.043 ± 0.004
325-326	25.09		63 ± 3	10.9 ± 0.4	38.8 ± 1.4	
335-336	27.82	2.68 ± 0.11	66 ± 3	11.2 ± 1.1	41.3 ± 1.6	0.046 ± 0.005
345-346	30.56	2.5 ± 0.3	65 ± 4	10.7 ± 0.8	40 ± 2	0.042 ± 0.009
355-356	31.78	2.6 ± 0.2	59 ± 3	10.6 ± 0.6	33 ± 2	0.057 ± 0.008
365-366	33.00	2.43 ± 0.13	59 ± 2	9.7 ± 0.4	34.3 ± 1.2	0.050 ± 0.005
375-376	34.22	2.77 ± 0.09	70 ± 4	11.3 ± 0.7	55 ± 3	0.041 ± 0.005
385-386	35.44	2.32 ± 0.11	63 ± 3	10.2 ± 0.4	37.9 ± 1.3	0.042 ± 0.005
395-396	36.66	2.09 ± 0.07	62 ± 2	10.0 ± 0.4	37.1 ± 1.3	0.035 ± 0.003
405-406	37.88	2.57 ± 0.09	63 ± 3	10.2 ± 0.4	40.7 ± 1.4	0.049 ± 0.005
435-436	41.38	2.16 ± 0.07	56 ± 2	9.9 ± 0.4	30.2 ± 1.1	0.049 ± 0.004
465-466	44.89	2.11 ± 0.07	58 ± 2	10.8 ± 0.4	28.4 ± 1.0	0.048 ± 0.004

* MD02-2594 age model based on ^{14}C AMS dates in *G. inflata* [Martínez-Méndez *et al.*, in revision].

Measured concentrations of ^{230}Th and ^{231}Pa in marine sediments consist of three fractions: isotopes scavenged from seawater; those supported by detrital U; and those produced by the decay of authigenic U. The ^{231}Pa/^{230}Th ratio used as a palaeoceanographic proxy is based entirely on the scavenged fraction (non-supported or excess fraction: $^{231}Pa_{xs}$), and thus, for the influence of the other two fractions must be corrected for:

$$A^{231}\mathrm{Pa}_{\mathrm{xs}} = A^{231}\mathrm{Pa}_{\mathrm{meas}} - A^{231}\mathrm{Pa}_{\mathrm{det}} - A^{231}\mathrm{Pa}_{\mathrm{auth}} \quad (1)$$

$$A^{230}\mathrm{Th}_{\mathrm{xs}} = A^{230}\mathrm{Th}_{\mathrm{meas}} - A^{230}\mathrm{Th}_{\mathrm{det}} - A^{230}\mathrm{Th}_{\mathrm{auth}} \quad (2)$$

Where *A* is activity and the subscripts

xs	excess (scavenged)
meas	measured (total)
det	detritic (continental origin)
auth	authigenic (from in situ ingrowth of U)

Detrital Component

The detrital fraction is contained in the mineral fraction derived from continental erosion and transported to the ocean by eolian, ice-rafted and riverine inputs. In the lithogenic fraction it is generally accepted that detrital ^{230}Th and ^{231}Pa are in secular equilibrium with their decay-chain predecessors, detrital ^{238}U and ^{235}U:

$$A^{230}\mathrm{Th}_{\mathrm{det}} = A^{238}\mathrm{U}_{\mathrm{det}} \quad (3)$$

$$A^{231}\mathrm{Pa}_{\mathrm{det}} = A^{235}\mathrm{U}_{\mathrm{det}} \quad (4)$$

The activity of detrital ^{238}U is estimated from the activity of ^{232}Th in sediment, which is entirely of lithogenic origin (Brewer *et al.*, 1980). Based on Walter *et al.*, (1997) and from own observations, Henderson and Anderson (2003) suggested a lithogenic ^{238}U/^{232}Th activity ratio of 0.6 ± 0.1 for the Atlantic Ocean.

$$A^{230}\mathrm{Th}_{\mathrm{det}} = A^{232}\mathrm{Th}_{\mathrm{meas}}\left(\frac{A^{238}\mathrm{U}}{A^{232}\mathrm{Th}}\right)_{\mathrm{Atlantic}} \quad (5)$$

The activity of detrital ^{235}U is estimated from the average natural ^{235}U/^{238}U activity ratio, 0.046.

$$A^{231}\mathrm{Pa}_{\mathrm{det}} = 0.046 \times A^{232}\mathrm{Th}_{\mathrm{meas}}\left(\frac{A^{238}\mathrm{U}}{A^{232}\mathrm{Th}}\right)_{\mathrm{Atlantic}} \quad (6)$$

Authigenic Component

The authigenic fraction is derived from the *in situ* ingrowth of ^{231}Pa and ^{230}Th resulting from the decay of the authigenic ^{235}U and ^{234}U in the sediment. The sediments studied are younger than 150 ka BP for an optimum estimation of ^{231}Pa/^{230}Th and hence, the precipitated U is not in secular equilibrium with their daughter nuclides yet. Therefore, authigenic ^{231}Pa and ^{230}Th have to be calculated applying the law of radioactive decay:

$$A^{230}\mathrm{Th}_{\mathrm{auth}} = A^{234}\mathrm{U}_{\mathrm{auth}}\left(1 - e^{-\lambda_{230Th}t}\right) \quad (7)$$

$$A^{231}\mathrm{Pa}_{\mathrm{auth}} = A^{235}\mathrm{U}_{\mathrm{auth}}\left(1 - e^{-\lambda_{231Pa}t}\right) \quad (8)$$

where λ is the decay constant (λ^{230}Th = 9.16 × 10^{-6} a^{-1}; λ^{231}Pa = 2.12 × 10^{-5} a^{-1}) and t is the time elapsed since the emplacement of authigenic U, which typically is taken as the time of deposition of the sediment layer from which the U is isolated.

Instead of measuring ^{234}U directly, it is calculated from ^{238}U, which is more abundant in nature and can be more accurately quantified. We estimate authigenic ^{238}U from the difference:

$$A^{238}\mathrm{U}_{\mathrm{auth}} = A^{238}\mathrm{U}_{\mathrm{meas}} - A^{238}\mathrm{U}_{\mathrm{det}} \quad (9)$$

Since authigenic U is derived from seawater, it is assumed to have an initial ^{234}U/^{238}U activity ratio of 1.146, equivalent to that of U dissolved in seawater (Chen *et al.*, 1986). Because all the samples analysed in this study are much younger than the ^{234}U half-life of 245 kyr, this ^{234}U/^{238}U activity ratio has been assumed to remain constant after sediment deposition. Combining (7) and (9):

$$A^{230}\mathrm{Th}_{\mathrm{auth}} = 1.146\left(A^{238}\mathrm{U}_{\mathrm{meas}} - A^{238}\mathrm{U}_{\mathrm{det}}\right)\left(1 - e^{-\lambda_{230Th}t}\right) \quad (10)$$

Calculation of ^{231}Pa$_{\mathrm{auth}}$ requires the natural ^{235}U/^{238}U activity ratio:

$$A^{231}\mathrm{Pa}_{\mathrm{auth}} = 0.046\left(A^{238}\mathrm{U}_{\mathrm{meas}} - A^{238}\mathrm{U}_{\mathrm{det}}\right)\left(1 - e^{-\lambda_{231Pa}t}\right) \quad (11)$$

Substituting ^{238}U$_{\mathrm{det}}$ by (5) and (6):

$$A^{230}\mathrm{Th}_{\mathrm{auth}} = 1.146\left[A^{238}\mathrm{U}_{\mathrm{meas}} - A^{232}\mathrm{Th}_{\mathrm{meas}}\left(\frac{A^{238}\mathrm{U}}{A^{232}\mathrm{Th}}\right)_{\mathrm{Atlantic}}\right]\left(1 - e^{-\lambda_{230Th}t}\right) \quad (12)$$

$$A^{231}\mathrm{Pa}_{\mathrm{auth}} = 0.046\left[A^{238}\mathrm{U}_{\mathrm{meas}} - A^{232}\mathrm{Th}_{\mathrm{meas}}\left(\frac{A^{238}\mathrm{U}}{A^{232}\mathrm{Th}}\right)_{\mathrm{Atlantic}}\right]\left(1 - e^{-\lambda_{231Pa}t}\right) \quad (13)$$

General Equation

The general equation to calculate scavenged ^{230}Th and ^{231}Pa in sediments, corrected for detrital and authigenic components, is thus:

$$A^{230}\mathrm{Th}_{\mathrm{xs}} = \left\{A^{230}\mathrm{Th}_{\mathrm{meas}}\right\} - \left\{A^{232}\mathrm{Th}_{\mathrm{meas}}\left(\frac{A^{238}\mathrm{U}}{A^{232}\mathrm{Th}}\right)_{\mathrm{Atlantic}}\right\} - \left\{1.146\left[A^{238}\mathrm{U}_{\mathrm{meas}} - A^{232}\mathrm{Th}_{\mathrm{meas}}\left(\frac{A^{238}\mathrm{U}}{A^{232}\mathrm{Th}}\right)_{\mathrm{Atlantic}}\right]\left(1 - e^{-\lambda_{230Th}t}\right)\right\} \quad (14)$$

$$A^{231}\mathrm{Pa}_{\mathrm{xs}} = \left\{A^{231}\mathrm{Pa}_{\mathrm{meas}}\right\} - \left\{0.046\,A^{232}\mathrm{Th}_{\mathrm{meas}}\left(\frac{A^{238}\mathrm{U}}{A^{232}\mathrm{Th}}\right)_{\mathrm{Atlantic}}\right\} - \left\{0.046\left[A^{238}\mathrm{U}_{\mathrm{meas}} - A^{232}\mathrm{Th}_{\mathrm{meas}}\left(\frac{A^{238}\mathrm{U}}{A^{232}\mathrm{Th}}\right)_{\mathrm{Atlantic}}\right]\left(1 - e^{-\lambda_{231Pa}t}\right)\right\} \quad (15)$$

Age Correction

Finally, information on sediment age is required to correct for the decay of excess ^{230}Th and ^{231}Pa since its deposition at the seafloor. This correction is given by:

$$A^{230}\mathrm{Th}_{\mathrm{xs},0} = A^{230}\mathrm{Th}_{\mathrm{xs}} \times e^{\lambda_{230Th}t} \quad (16)$$

$$A^{231}\mathrm{Pa}_{\mathrm{xs},0} = A^{231}\mathrm{Pa}_{\mathrm{xs}} \times e^{\lambda_{231Pa}t} \quad (17)$$

S3: Influence of particle fluxes on sedimentary $^{231}Pa/^{230}Th$ south of MD02-2594.

In addition to MD02-2594 (34º42.64' S; 17º20'32 E; 2,440m water depth), continuous down-core analyses were carried out on core MD02-2588, located further to the south (41.12ºS; 25.30ºE; 2,907m), in order to test the potential influence of particle fluxes on $^{231}Pa/^{230}Th$ ratios in the region. In order to broaden the geographic coverage, spot measurements were performed on two additional sediment cores: TN057-21-PC2 (41º08'S, 7º49'E; 4,981m) and PS2489-2PC (42º52.4 S, 8º58.4 E; 3,794 m). The geographic location of the cores is shown in Figure S1.1 and the results in Figure S1.2.

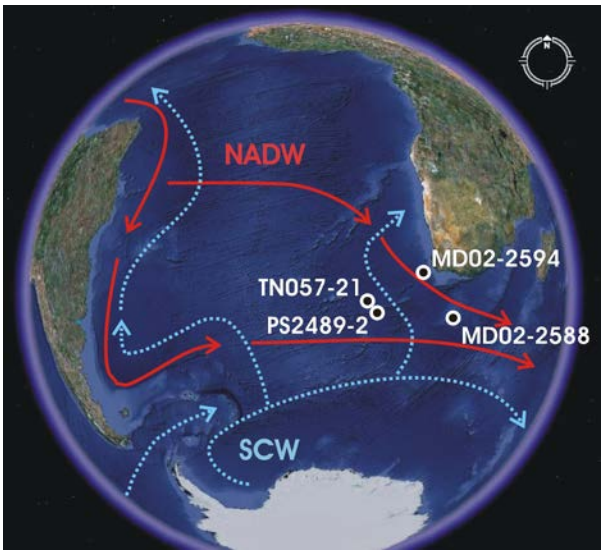

Figure S3-1. Location of cores MD02-2594 and MD02-2588 in the Agulhas Corridor, and TN057-21 and PS2489-2 in the open South Atlantic. Labels indicate main water mass contributors, North Atlantic Deep Water (NADW) and Southern Component Waters (SCW). Schematic main water mass pathways at present are indicated with arrows (NADW red, SCW light dotted blue) and are based on Arhan *et al*. (2003). Background image from Google Earth.

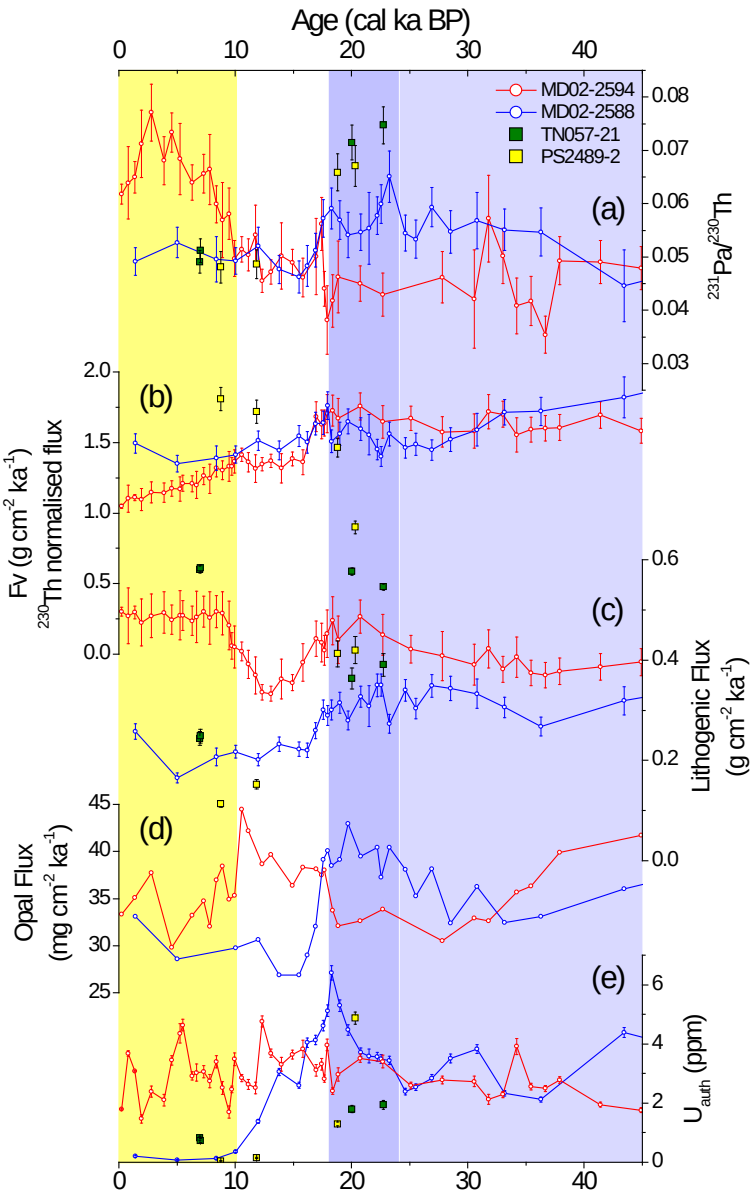

Figure S3-2. Multi-proxy record profiles of cores MD02-2594 (presented in the main text) and MD02-2588 (presented only in the SI), and spot measurements of TN057-21 and PS2489-2, showing (a) ^{231}Pa/^{230}Th ratios, (b) ^{230}Th-normalised total particle flux (*Fv*), (c) ^{230}Th-normalised lithogenic flux record, (d) ^{230}Th-normalised opal flux, and (e) authigenic uranium concentration. Error bars indicate analytical s.d. Vertical shading highlights time intervals: Holocene (0-10 ka BP), yellow; T1 (10-18 ka BP), white; LGM (18-24 ka BP), blue; glacial stages MIS 2 and late MIS 3, light blue). The decrease of ^{231}Pa/^{230}Th in MD02-2588 at the end of the last glacial is paralleled by a decrease in opal flux, and to a lesser extent in the lithogenic fraction and the authigenic uranium. This potentially suggests that sedimentary ^{231}Pa/^{230}Th is reflecting primarily a change in particle settling flux and associated Pa scavenging rather than changes in

lateral water mass advection. This also appears to be the case for cores PS2489 and TN057-21 that consistently display higher LGM $^{231}Pa/^{230}Th$ ratios and particle fluxes. These results strongly suggest that varying particle composition, opal in particular, is a major factor defining the sedimentary $^{231}Pa/^{230}Th$ signal in MD02-2588. The glacial to Holocene decrease of $^{231}Pa/^{230}Th$ ratios and opal fluxes in MD02-2588, and also in TN057-21 and PS2489, seem consistent features accompanying the shift of the opal belt to the south. This conclusion fits well with a previous study suggesting that the latitudinal $^{231}Pa/^{230}Th$ gradient in the region also shifted to the south during the last glacial-interglacial transition (Kumar *et al.*, 1995). The results from MD02-2594 indicate that variable settling particle fluxes are not the dominant control on $^{231}Pa/^{230}Th$ ratios in this site, hence plausibly reflect changes in the deep water circulation.

S4: Complementary $^{231}Pa/^{230}Th$ data from the equatorial Atlantic (Bradtmiller *et al.*, 2007).

We provide below a version of Figure 2 of the manuscript including $^{231}Pa/^{230}Th$ data published in Bradtmiller *et al.* (2007) from the equatorial Atlantic. The Bradtmiller data for the LGM would be consistent with our interpretation, with $^{231}Pa/^{230}Th$ values falling in between those of our new core and existing North Atlantic records (as would be expected for a gradual increase in $^{231}Pa/^{230}Th$ as water flows northward). These data is therefore consistent with our proposed explanation of the LGM and could, in fact, be taken as strong support for our case. We chose not to make this argument in the manuscript, however, because the effect of opal flux changes on $^{231}Pa/^{230}Th$ records is evident for the Bradtmiller data in a core by core basis.

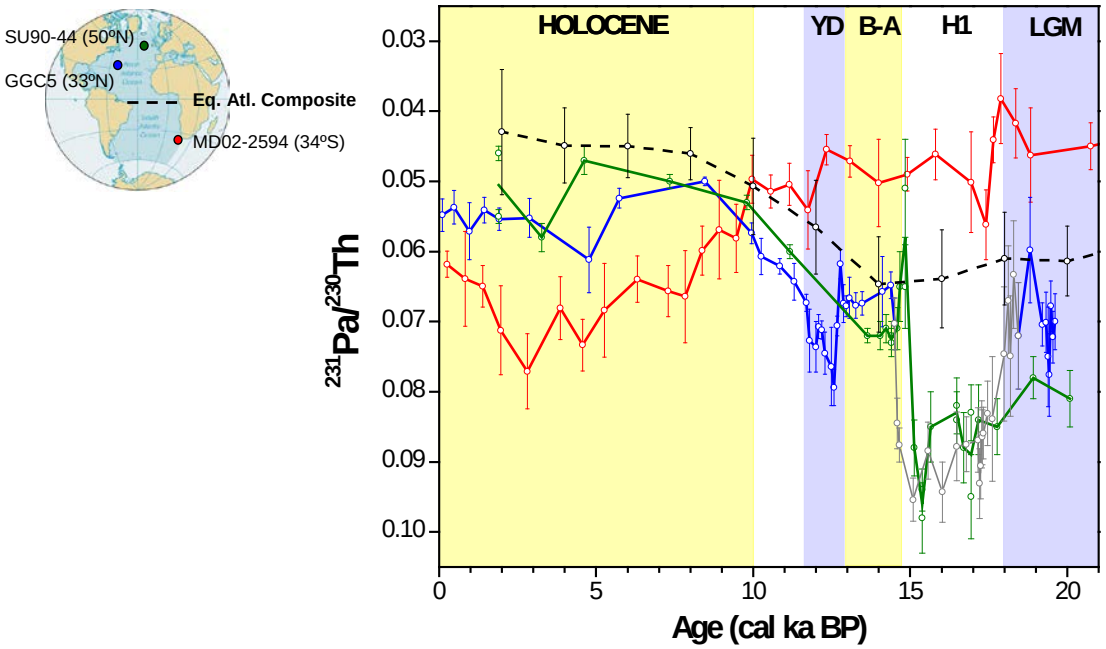

Figure S4-1. Alternative Figure 2, showing data of Bradtmiller et al. (2007) as a black dashed line (the curve represents the mean of the seven cores that study presented - error bars along the record are s.e.m.). Other records: MD02-2594 from our study in red, and the North Atlantic GGC5 from McManus et al. (2004) in blue, and the SU90-44 from Gherardi et al. (2009) in blue; these are shown with analytical s.d.

References in Supplementary Information

Arhan, M., Mercier, H. & Park, Y.-H. On the deep water circulation of the eastern South Atlantic Ocean. *Deep-Sea Res.* **50**, 889-916 (2003).

Brewer, P.G., Nozaki, Y., Spencer, D.W. & Fleer, A.P. Sediment trap experiments in the deep North Atlantic: isotopic and elemental fluxes. *J. Mar. Res.* **38**, 703-728 (1980).

Chen, J.H., Edwards, R.L. & Wasserburg, G.J. ^{238}U, ^{234}U and ^{232}Th in seawater. *Earth Planet. Sc. Lett.* **80**, 241-251 (1986).

Gherardi, J.-M. *et al.* Glacial-interglacial circulation changes inferred from ^{231}Pa/^{230}Th sedimentary record in the North Atlantic region. *Paleoceanography* **24**, PA2204, doi:10.1029/2008PA001696 (2009).

Henderson, G.M. & Anderson, R.F. The U-series toolbox for paleoceanography. *Rev. Mineral. Geochem.* **52**, 493-531 (2003).

Kumar, N. *et al.* Increased biological productivity and export production in the glacial Southern Ocean. *Nature* **378**, 675-680 (1995).

Marchal, O., Francois, R., Stocker, T.F. & Joos, F. Ocean thermohaline circulation and sedimentary ^{231}Pa/^{230}Th ratio. *Paleoceanography* **15**, 625-641 (2000).

Martínez-Méndez, G. *et al.* Contrasting multi-proxy reconstructions of surface ocean hydrography in the Agulhas Corridor and implications for the Agulhas Leakage during the last 345,000 years. *Paleoceanography*, in revision.

McManus, J.F., Francois, R., Gherardi, J.-M., Keigwin, L.D. & Brown-Leger, S. Collapse and rapid resumption of Atlantic meridional circulation linked to deglacial climate changes. *Nature* **428**, 834-837 (2004).

Thomas, A.L., Henderson, G.M. & McCave, I.N. Constant bottom water flow into the Indian Ocean for the past 140 ka indicated by sediment $^{231}Pa/^{230}Th$ ratios. *Paleoceanography* **22**, PA4210, doi:10.1029/2007PA001415 (2007).

Walter, H.-J., Rutgers van der Loeff, M.M. & Hoeltzen, H. Enhanced scavenging of ^{231}Pa relative to ^{230}Th in the South Atlantic south of the Polar Front: Implications for the use of the $^{231}Pa/^{230}Th$ ratio as a paleoproductivity proxy. *Earth Planet. Sc. Lett.* **149**, 85-100 (1997).

Yu, E.F., François, R. & Bacon, M.P. Similar rates of modern and last-glacial ocean thermohaline circulation inferred from radiochemical data. *Nature* **379**, 689-694 (1996).